Mutations in the Rod Outer Segment Membrane Guanylate Cyclase in a Cone−Rod Dystrophy Cause Defects in Calcium Signaling†

Teresa Duda,*,‡ Anuradha Krishnan,‡ Venkateswar Venkataraman,‡ Christian Lange,§ Karl-Wilhelm Koch,§ and Rameshwar K. Sharma‡

The Unit of Regulatory and Molecular Biology, Departments of Cell Biology and Ophthalmology, New Jersey Medical School, University of Medicine and Dentistry of New Jersey, Stratford, New Jersey 08084, and Institut fur Biologische Informationverarbeitung, Forschungszentrum Julich, Postfach 1913, D-52425 Julich, Germany

Received July 9, 1999; Revised Manuscript Received August 20, 1999

ABSTRACT: Rod outer segment guanylate cyclase 1 (ROS-GC1) is a member of the subfamily of Ca^{2+}-regulated membrane guanylate cyclases; and it is pivotal for vertebrate phototransduction. Two opposing regulatory modes control the activity of ROS-GC1. At nanomolar concentrations of Ca^{2+}, ROS-GC1 is activated by Ca^{2+}-binding proteins named guanylate cyclase activating proteins (GCAPs). However, at micromolar concentrations of Ca^{2+}, ROS-GC1 is stimulated by S100β [also named calcium-dependent (CD) GCAP]. This mode is not linked with phototransduction; instead, it is predicted to be involved in retinal synaptic activity. Two point mutations, E786D and R787C, in ROS-GC1 have been connected with cone−rod dystrophy (CORD6), with only one type of point mutation occurring in each family. The present study shows that the E786D mutation has no effect on the basal catalytic activity of ROS-GC1 and on its activation by GCAP1 and S100β; however, the mutated cyclase becomes more activated by GCAP2. The R787C mutation has three consequences: (1) it causes major damage to the basal cyclase activity, (2) it makes the cyclase 5-fold more sensitive to activation by GCAP1; and 3) converts the cyclase into a form that is less sensitive to activation by GCAP2 and S100β. Thus, the two CORD6-linked mutations in ROS-GC1, which occur at adjacent positions, result in vastly different biochemical phenotypes, and they are connected with very specific molecular defects in the Ca^{2+} switching components of the cyclase. These defects, in turn, are proposed to have a profound effect on both the machinery of phototransduction and the retinal synapse. The study for the first time defines the biochemistry of CORD6 pathology in precise molecular terms.

Vertebrate rods and cones are highly differentiated retinal neurons that generate electric signals in response to captured photons. The biochemical process by which these signals are generated is called phototransduction (reviewed in refs *1* and *2*). Two pivotal molecules of phototransduction are Ca^{2+} and cyclic GMP, which are interlocked in a reciprocal feedback loop (*3*, *4*). The captured photon causes a decline in the level of cyclic GMP and closure of the cyclic GMP-gated cation channels. This results in the lowering of intracellular Ca^{2+} from ∼500 nM in dark-adapted photoreceptor cell to below 100 nM after illumination (*5*−*9*). The decrease of intracellular Ca^{2+} activates the rod outer segment (ROS)[1] membrane guanylate cyclase (ROS-GC1). Increased synthesis of cyclic GMP along with the inactivation of the phototransduction cascade leads to the reopening of the cyclic GMP-gated channels and restoration of the dark current of the photoreceptors.

Four subtypes of membrane guanylate cyclases have been cloned from the retina. Two are peptide receptors and two are not. The peptide receptors, ANF-RGC (*10*, *11*) and CNP-RGC (*12*), have no role in phototransduction (2). The non-peptide receptors, ROS-GC1 (*13*, *14*; structure in ref *15* corrected in GenBank accession no. M92432) and ROS-GC2 (*14*, *16*, *17*), belong to the subfamily of ROS-GC. They reside in photoreceptors and mimic the native cyclase activity under conditions of phototransduction, i.e., their cyclase activities are cooperatively activated by low Ca^{2+}, with $K_{1/2}$ near 100 nM, and are progressively inhibited with increasing Ca^{2+} concentrations (*16*−*18*). Hence, they are regulated intracellularly by Ca^{2+} and meet the criterion of being linked with phototransduction (*3*). The physiological significance of the heterogeneity in ROS-GCs and its relationship with

† This study was supported by USHPS awards EY 10828 (R.K.S.) and HL 58151 (T.D.); by the affiliated support of the Research to Prevent Blindness Inc., New York; the Lions Eye Research Foundation, New Jersey, by the facilities provided by UMDNJ-SOM; and by an award from the Deutsche Forschungsgemeinschaft (K.-W.K.).

* Author to whom correspondence should be addressed: Phone 609-566-6976; Fax 609-566-7057; Email dudatm@pearl.umdnj.edu.

‡ University of Medicine and Dentistry of New Jersey.

§ Forschungszentrum Julich.

[1] Abbreviations: ANF-RGC, atrial natriuretic factor receptor guanylate cyclase; BSA, bovine serum albumin; CD-GCAP, calcium-dependent guanylate cyclase activating protein; CNP-RGC, C-type natriuretic peptide receptor guanylate cyclase; CORD, cone−rod dystrophy; EGTA, ethylene glycol bis(β-aminoethyl ether)-*N*,*N*,*N*′,*N*′-tetraacetic acid; GCAP, guanylate cyclase activating protein; GTP, guanosine 5′-triphosphate; LCA, Leber's congenital amaurosis; MOPS, 3′-(*N*-morpholino)propanesulfonic acid; ROS, rod outer segment; ROS-GC, rod outer segment guanylate cyclase; SDS, sodium dodecyl sulfate; SDS−PAGE, sodium dodecyl sulfate−polyacrylamide gel electrophoresis; SPR, surface plasmon resonance; wt-r, wild type recombinant.

10.1021/bi9915972 CCC: $18.00
Published on Web 09/30/1999

rod−cone expression pattern is not known. However, the emerging evidence strongly supports the physiological linkage of ROS-GC1 with phototransduction in ROS: (1) To date, only ROS-GC1 presence in ROS has been demonstrated biochemically via its purification from ROS and partial sequencing (*19*, *20*); (2) mutations that cause loss of ROS-GC1 expression lead to defects in retinal morphology as well as visual transduction in human (*21*) and chicken (*22*); and (3) only ROS-GC1 mutations specific to a rod-specific abnormality, Leber's congenital amaurosis (LCA1) (*21*), explain the disease phenotype in molecular terms (*23*).

A recent study has mapped two mutations, collectively termed cone−rod dystrophy type 6 (CORD6), to human chromosome 17p12-p13, where the gene of ROS-GC1 is also localized (*24*). Each mutation is linked with a single amino acid substitution in ROS-GC1: E786D or R787C in an individual patient (*24*). Typical phenotypic characteristics of CORD-linked diseases are that they first cause deterioration of cone photoreceptor cells and then of rod photoreceptor cells (*24*). Thus, the disease damages both cones and rods: At the early stage of the disease, there is photophobia and loss of color vision, followed by night blindness and macular degeneration at the later stage (*24*). Hence, ROS-GC1 is linked not only with rod-specific phototransduction but also with cone-specific phototransduction.

In line with the membrane guanylate cyclase family trait, ROS-GC1 is a single transmembrane-spanning protein with an extracellular segment and an intracellular segment of almost equal length (*13*). A 26 amino acid transmembrane domain partitions the two segments (*13*−*15*). The intracellular domain is composed of modular blocks and contains at least three distinct Ca^{2+} signaling modules, which regulate the core catalytic cyclase module (model in Figure 6 of ref *25*). Regulation by Ca^{2+} is indirect, via Ca^{2+}-binding proteins: two isoforms of guanylate cyclase activating protein, GCAP1 and GCAP2, activate ROS-GC1 at 100 nM free Ca^{2+} or below (*26*−*30*); a different type of Ca^{2+}-binding protein, S100β, also termed as CD-GCAP, activates ROS-GC1 at micromolar free Ca^{2+} (*31*−*33*). Regulation by GCAPs is linked with phototransduction (*18*, *25*, *27*), whereas regulation by S100β is presumably linked with retinal synaptic activity (*31*−*33*).

The present study was undertaken to analyze the effect of the two CORD6-linked mutations on the phototransduction- and/or synaptic-linked components of ROS-GC1 and thus to define the biochemistry of the CORD6 pathology in precise molecular terms.

MATERIALS AND METHODS

Construction of ROS-GC1 Mutants. Two CORD6-related ROS-GC1 mutants, E786D and R787C, were constructed. The numbering corresponds to the mature ROS-GC1 protein (*13*). Both mutations required a single nucleotide change. The GAG codon for glutamic acid was changed to the GAC codon for aspartic acid, and the CGC codon for arginine was changed to the TGC codon for cysteine. The mutations were introduced by the technique of coupled priming mutagenesis (*18*, *23*) with the ampicillin-repair primer (for selection) and the following mutagenic primers: 5′-GACCTGATCCGGGA**C**CGCACAGAGGA for E786D, and 5′-CTGATCCGGGAG**T**GCACAGAGGAGCT-3′ for R787C (the mutated nucleotides are in boldface type and underlined). The mutated recombinants were sequenced to confirm their identities. They were then individually subcloned into a pcDNA3 expression vector (Invitrogen).

Insertion of N-Terminal FLAG Epitope into ROS-GC1 and Its Mutants. FLAG (DYKDDDDK) epitope was inserted into ROS-GC1 immediately after the signal peptide cleavage site (*13*, *23*). The construct is named FLAG-ROS-GC1. FLAG-E786D and FLAG-R787C ROS-GC1 mutants were built by substituting the *Sfi*I/*Bam*HI fragment of FLAG-ROS-GC1 cDNA in pcDNA3 expression vector with the *Sfi*I/*Bam*HI fragment of the ROS-GC1 mutants.

Expression and Purification of Recombinant GCAP1 and GCAP2. The bovine GCAP1 cDNA was expressed in *Escherichia coli* ER2566 strain carrying the plasmid pBB131 (a kind gift of Dr. J. Gordon) encoding yeast N-myristoyltransferase. The protein was purified as described previously (*23*). The bovine GCAP2 cDNA was expressed in Sf9 insect cells and purified to homogeneity as described in ref *34*.

Expression Studies. COS-7 cells (simian virus 40-transformed African green monkey kidney cells), maintained in Dulbecco's modified Eagle's medium with penicillin, streptomycin, and 10% fetal bovine serum, were transfected with the expression constructs by the calcium phosphate coprecipitation technique (*35*). Sixty hours after transfection, cells were washed twice with 50 mM Tris-HCl (pH 7.5)/10 mM $MgCl_2$ buffer, scraped into 2 mL of cold buffer, homogenized, centrifuged for 15 min at 5000*g*, and washed several times with the same buffer; the pellet represented the crude membranes.

Guanylate Cyclase Assay. The crude membranes were assayed for guanylate cyclase activities as described previously (*36*). Briefly, the membranes were preincubated in an ice bath with or without GCAP1, GCAP2, or S100β in the assay system containing 10 mM theophylline, 15 mM phosphocreatine, 20 μg of creatine kinase, and 50 mM Tris-HCl (pH 7.5) and adjusted to the appropriate free Ca^{2+} concentrations with precalibrated Ca^{2+}/EGTA solutions (Molecular Probes). Total assay volume was 25 μL. The reaction was initiated by the addition of the substrate solution containing 4 mM $MgCl_2$ and 1 mM GTP. Incubation (37 °C, 10 min) was terminated by the addition of 225 μL of 50 mM sodium acetate buffer (pH 6.2) followed by heating in a boiling water bath for 3 min. The amount of cyclic GMP formed was determined by radioimmunoassay (*37*).

Western Blot. After boiling in gel-loading buffer [62.5 mM Tris-HCl, (pH 7.5), 2% SDS, 5% glycerol, 1 mM β-mercaptoethanol and 0.005% bromophenol blue], 20 μg of membrane protein was subjected to sodium dodecyl sulfate−polyacrylamide gel electrophoresis (SDS−PAGE) in a buffer (pH 8.3) containing 0.025 M Tris, 0.192 M glycine, and 0.1% SDS. The proteins were transferred to Immobilon membranes (Millipore) in the same buffer but containing 5% methanol. The blot was incubated in Tris-buffered saline (TBS, pH 7.5) containing 100 mM Tris-HCl, 0.9% NaCl, and 0.05% Tween-20 (TBS-T) with 5% powdered nonfat Carnation milk (blocking buffer) overnight at 4 °C and rinsed with TBS-T. The anti-FLAG monoclonal antibodies (Sigma) were added at 1:300 dilution in the blocking buffer and the incubation was continued for 1 h. After the blot was rinsed with TBS-T, the incubation was continued with the secondary antibody conjugated to horseradish peroxidase in blocking

buffer (1:20 000) for another hour. Finally the blot was treated with SuperSignal blaze chemiluminescent substrate (Pierce) for 5 min according to the manufacturer's protocol. The immunoreactive band was detected by exposing the blot to Kodak X-ray film for 15 s.

Surface Plasmon Resonance Measurements. SPR spectroscopy was applied to test interaction between peptides that encompass the region surrounding amino acid (aa) residues 786 and 787 of ROS-GC1 and the Ca^{2+}-binding proteins GCAP1, GCAP2, and S100β. Peptides representing the region aa 744−807 in bovine ROS-GC1 were synthesized with a multipin peptide synthesis kit (Chiron Mimotopes). The manufacturer's protocol was modified according to ref *38*. Each peptide was 12 aa long and overlapped with the preceding one by 10 amino acids. The peptides were numbered 54−80, according to an internal laboratory system. Binding of peptides to GCAP1, GCAP2, and S100β was tested by recording sensograms with a BIAcore system using BIAcore control software 1.2. Each Ca^{2+}-binding protein was immobilized on the surface of a dextran-coated sensor chip via a cysteine thiol group as described previously (*39*). Immobilization levels were 0.3 pmol/mm^2 for GCAP1 and GCAP2 and 0.4 pmol/mm^2 for S100β. A control surface was made by immobilizing cysteine. Peptides were dissolved or suspended in running buffer (40 mM MOPS, pH 7.1, 60 mM KCl, 10 mM NaCl, 10 mM $MgCl_2$, 0.005% Tween 20, and 0.01% BSA) and 2 mM ethylene glycol bis(β-aminoethyl ether)-*N*,*N*,*N*′,*N*′-tetraacetic acid (EGTA) ($-Ca^{2+}$) or 2 mM Ca-EGTA ($+Ca^{2+}$) as indicated. Free Ca^{2+} concentration was adjusted and calculated as described previously (*39*): solutions labeled $-Ca^{2+}$ contained 1 nM free Ca^{2+}, and solutions labeled $+Ca^{2+}$ contained 24 μM free Ca^{2+}. The concentration of peptides was 0.5 mg/mL (approximately 0.3 mM). Undissolved material was removed by a short centrifugation step (5 min, 15000*g*) and the supernatant was used to monitor interaction with immobilized GCAP1 (GCAP2 or S100β) as described below. The flow rate was set at 5 μL/min. The flow cell was equilibrated with running buffer for 10 min before a normalization pulse of 1% glycerol in running buffer was applied. After further equilibration for 10 min, 20 μL of a peptide solution was injected and the resonance signal was recorded at the end of the injection. Peptide solutions were injected over a surface coated with GCAP1, GCAP2, or S100β and over a control surface, where cysteine had been immobilized. The surface was then regenerated with a pulse of 10 μL of 0.5% sodium dodecyl sulfate (SDS), followed by 10 μL of 0.1 M $CaCl_2$. Changes in resonance signal evoked by the peptide injection were normalized to the 1% glycerol pulse. The normalized specific response was then calculated by subtracting the normalized response obtained with the control flow cell from the normalized response obtained with the GCAP1-, GCAP2-, or S100β-coated flow cell.

RESULTS

E786D Mutation in ROS-GC1 Does Not Affect Its Basal Cyclase Activity; R787C Mutation Damages It. CORD6 is heterogeneous. Two missense mutations in ROS-GC1 gene, E786D and R787C, have been linked with this disease in four British families (*24*). Each afflicted family contains only one of the above mutations. Both of these mutations are in exon 18 of the gene (*40*−*42*). The two residues, E786 and R787, are adjacent to each other and are invariant between its human, dog, rat, mouse, and bovine forms (Figure 1). Thus, they are conserved. To elucidate the biochemical consequences of the E786D and R787C mutations on the basal state of ROS-GC1, the mutations were created in the wild-type cloned ROS-GC1. The cyclases were expressed in a heterologous system of COS cells where, under native conditions, there is no expression of ROS-GC1. Leader sequence of all constructs was retained to ensure proper translocation and folding of the proteins. The cell membranes expressing the recombinant guanylate cyclases were tested for basal activity. To ensure that these activities are represented by equal amounts of the proteins, their expressions were assessed in parallel. A highly immunogenic FLAG epitope (DYKDDDDK) was inserted into the cyclases immediately after the signal peptide cleavage site (*13*). Insertion of FLAG sequence does not affect the basal cyclase activity (*23*). The FLAG constructs were expressed in COS cells. The membranes were subjected to a Western analysis with anti-FLAG monoclonal antibodies. The blots showed single immunoreactive bands of almost equal intensity (Figure 2B), indicating comparable expression of the proteins.

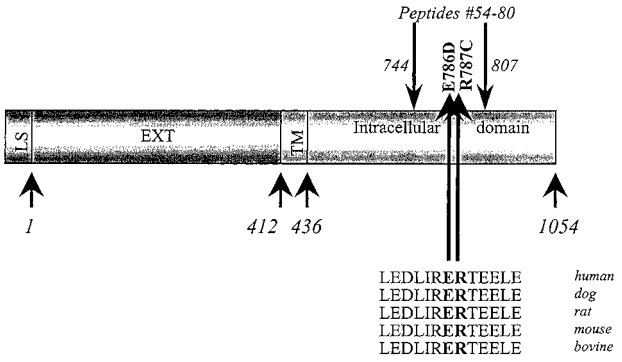

FIGURE 1: Schematic representation of the ROS-GC1 protein. The following denote the predicted domains: LS, leader sequence; EXT, extracellular (intradiscal) domain; TM, transmembrane domain. Numbers indicated correspond to the mature protein (*13*). Alignment of the human, dog, rat, mouse and bovine amino acid sequences (GenBank accession numbers M92432/AJ222657, Y15483, L36029, L41933, L37089, respectively) in the region surrounding positions 786 and 787 is shown. The location of overlapping peptides 54−80, used in binding experiments, is also indicated.

The basal guanylate cyclase activities of the wt-rROS-GC1 and E786D were almost equal, about 130 and 120 pmol of cyclic GMP min^{-1} (mg of protein)$^{-1}$, respectively (Figure 2A). Thus, the E786D mutation does not affect the basal activity of ROS-GC1.

The basal guanylate cyclase activity of the R787C mutant was about 30 pmol of cyclic GMP min^{-1} (mg of protein)$^{-1}$, which was only about one-fourth the wt-rROS-GC1 activity (Figure 2A). This indicates that, in contrast to the E786D mutation, which has no influence, the R787C mutation causes a major loss in the intrinsic cyclase activity of ROS-GC1.

E786D and R787C Mutations Result in Different Responsiveness of ROS-GC1 to GCAP1 and GCAP2. GCAP1 and GCAP2 activate ROS-GC1 at low Ca^{2+} concentrations, but the target site in ROS-GC1 is different for GCAP1 and GCAP2 (*25*, *34*). To determine the biochemical consequences of E876D and R787C mutations under the Ca^{2+} concentration that mimics light-adapted photoreceptors, COS cell mem-

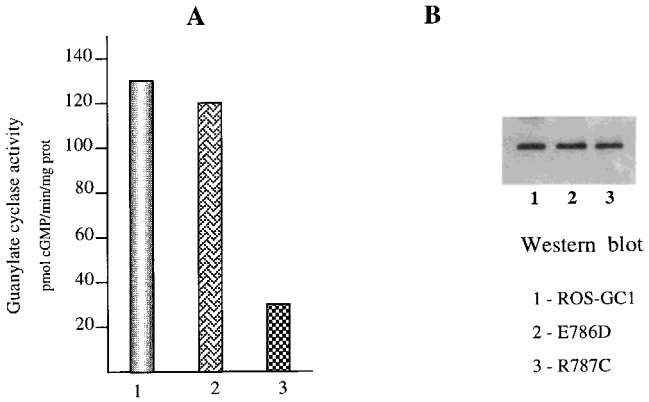

FIGURE 2: Expression of the wt-rROS-GC1, E786D, and R787D mutant proteins. (A) Guanylate cyclase activity. COS7 cells were individually transfected with the appropriate expression constructs, and the membranes were prepared as described under Materials and Methods. These were assayed for guanylate cyclase activity. The experiment was repeated three times for reproducibility. (B) Western blot. Proteins (20 μg of COS7 cell membranes containing FLAG-ROS-GC1, FLAG-E786D, or FLAG-R787C) were subjected to SDS−PAGE. After electrophoresis the proteins were transferred to Immobilon membranes, and the blots were incubated with anti-FLAG monoclonal antibody and with the secondary antibody as described under Materials and Methods. Immunoreactive bands were visualized by exposing the blots to Kodak X-ray film. The experiment was repeated three times with membranes prepared from separate transfection experiments.

branes expressing the wild type and the mutants were incubated with incremental concentrations of purified recombinant GCAP1 or GCAP2 at a fixed (10 nM) Ca^{2+} concentration. The membranes expressing wt-rROS-GC1 served as control.

GCAP1 stimulated the wild type and E786D in a dose-dependent fashion, with almost identical stimulatory patterns (Figure 3A). The maximal cyclase activation was about 5-fold over the basal value; the half-maximal effective concentration (EC_{50}) of GCAP1 was reached at about 1 μM, and saturation at about 3 μM. The results indicate that E786D mutation will not alter the light-adapted state of the photoreceptors.

In contrast to the E786D mutation, ROS-GC1 with the R787C mutation responded to saturating concentrations of GCAP1 with a 25-fold activation over the basal value (Figure 3A). Thus, the mutant was 5-fold more responsive to GCAP1 than the wild type. The EC_{50} value of GCAP1 for the mutant and the wild-type cyclase was the same, however. Therefore, the mutation converts ROS-GC1 into a state where it is 5-fold hyperactive to a GCAP1 signal.

E786D and R787C mutations showed opposite effects on GCAP2 regulation of ROS-GC1. Here, the former mutation converted ROS-GC1 into a form that was more responsive to GCAP2 at saturating concentrations (Figure 3B), and intriguingly, the R787C mutant was less responsive to GCAP2 (Figure 3B). There was no change in the EC_{50} value with any of the mutants. Thus, the mutations differentially alter the GCAP1- and GCAP2-mediated regulation of ROS-GC1.

To determine the biochemical consequences of the mutations on the dark- and light-adapted state of photoreceptors, Ca^{2+}-dependent modulation of cyclase activity was investigated at maximal GCAP1 or GCAP2 concentrations and at varying concentrations of Ca^{2+}. The pattern was identical for the wild-type and mutated cyclases (Figure 4A,B). The cyclase activity increased when the free Ca^{2+} concentration decreased. Half-maximal activation of ROS-GC1 by GCAP1 or GCAP2 was at about 120 nM free Ca^{2+}, irrespective whether the wild type or the mutants E786D and R787C were tested. Thus, the mutations do not alter the Ca^{2+} sensitivity of the switching mechanism; they only alter the activation process by GCAP1 and GCAP2.

E786D Mutation Does Not Alter the S100β-Mediated Activation of ROS-GC1; R787C Mutation Lowers It. Besides regulation by GCAPs (vide supra), ROS-GC1 is activated by S100β (CD-GCAP) at micromolar Ca^{2+} concentrations (*31*−*33*). To determine the biochemical consequences of E786D and R787C mutations on the regulation by S100β, the membranes expressing the mutants were incubated with incremental concentrations of S100β, at a fixed, high (1 mM) Ca^{2+} concentration. In parallel, under identical conditions, the membranes expressing wt-rROS-GC1 were analyzed. S100β stimulated wt-rROS-GC1 and both mutants in a dose-dependent fashion; in each case, half-maximal activation of the enzyme occurred at ~1 μM and saturation between 2

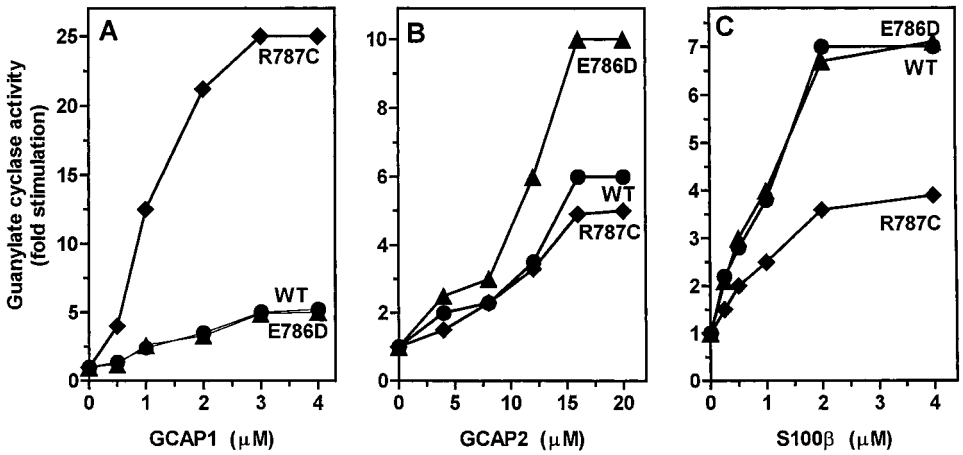

FIGURE 3: Effect of GCAP1 (A), GCAP2 (B), and S100β (C) on the cyclase activity of the wt-rROS-GC1 and mutant proteins E786D and R787C. COS7 cells were transfected with appropriate expression constructs and the membranes were prepared as described under Materials and Methods. These were assayed for guanylate cyclase activity in the presence of 10 nM Ca^{2+} and incremental concentrations of GCAP1 or GCAP2, and in the presence of 1 mM Ca^{2+} and indicated concentrations of S100β. Each experiment was done in triplicate and repeated at least three times with separate membrane preparations. The depicted curves are from one typical experiment. Error bars are within the sizes of the symbols.

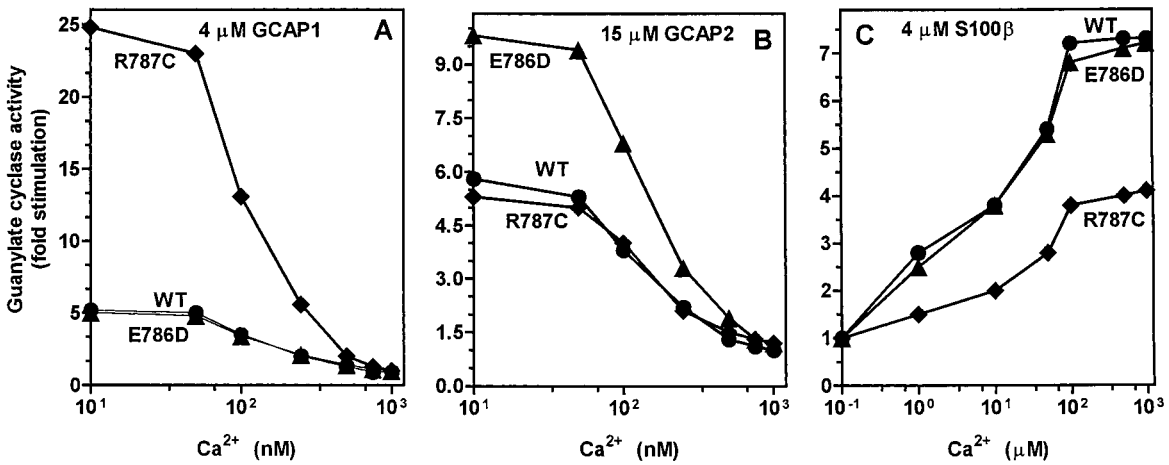

FIGURE 4: Ca^{2+} dependence of wt-rROS-GC1, E786D, and R787C guanylate cyclase activities in the presence of 4 μM GCAP1 (A), 15 μM GCAP2 (B), or 4 μM S100β (C). Membranes of COS7 cells expressing wt-rROS-GC1, E786D, or R787C were assayed for guanylate cyclase activity in the presence of saturating concentrations of GCAP1, GCAP2, or S100β and increasing concentrations of free Ca^{2+}. The results were normalized to the values presented in Figure 3. Each experiment was done in triplicate and repeated two times. The results presented are from one representative experiment. Error bars are within the sizes of the symbols.

and 4 μM (Figure 3C). The stimulation of all the cyclases was Ca^{2+}-dependent, with EC_{50} occurring at ~15 μM (Figure 4C). However, at saturating S100β concentration, R787C mutant was significantly less active than the wild type or the E786D mutant. Thus, the E786D mutation does not alter the S100β-dependent response. The R787C mutation, on the other hand, decreases it.

Region Encompassing the CORD6-Related Amino Acids Is Not Involved in Binding of GCAPs and S100β. Are E786D and R787C mutations in ROS-GC1 located in a region that directly binds GCAP1, GCAP2, or S100β? This issue was resolved by a surface plasmon resonance study.

GCAPs or S100β were individually immobilized on a sensor chip. Synthetic peptides covering the region aa 744−807 of ROS-GC1 (Figure 1) were applied in the mobile phase. Amino acids E786 and R787 are present in peptides 70−75 (peptide 70, ^{776}YSSNLEDLIR**ER**^{787}; peptide 75, ^{786}**ER**TEELELEKQK^{797}). The results are presented in Figure 5. No binding of GCAP1, GCAP2, or S100β was observed with peptides 65−80 **(**aa 766−807**)** in the absence or presence of Ca^{2+}. However, small responses were observed with peptides 56−59 (aa 748−765). In the case of GCAP1 and GCAP2 with peptides 56−59, the response signals were larger in the absence of Ca^{2+} than in the presence of Ca^{2+} (compare Figure 5 panels A and B). In the case of S100β with peptides 56−59, the binding signals were smaller under both Ca^{2+} conditions than the signals observed with GCAP1 and GCAP2; however, the binding responses were slightly larger in the presence of Ca^{2+}. As a positive control for binding we used a peptide from the intracellular region, ^{507}DWVWLKK**F**PGDR^{518}. This peptide contains a phenylalanine at position 514 that is mutated to a serine in the retinal disease LCA1 (*21*). The mutated ROS-GC1 is not activated by GCAP1 (*23*), indicating that this region is critical for regulation by GCAP1 and a possible site for interaction. Binding of GCAP1 to this peptide was observed by SPR spectroscopy with a 3−4-fold higher amplitude of the response signals than binding to peptides 56−59 (data not shown). Binding of GCAP1 to ROS-GC1 probably occurs via a multipoint attachment including the sites represented by these peptides (D507−R518 and 56−59). We conclude from these results that the CORD6-related amino acids are not located within the binding sites for GCAPs or S100β.

DISCUSSION

In this study an attempt has been made to define the biochemistry behind the pathology of two types of CORD6 in molecular terms. Both CORDs are the direct consequences of ROS-GC1 mutations. One involves E786D, and the other, R787C (*24*). ROS-GC1 is a pivotal molecule of phototransduction machinery and also, seemingly, of retinal synaptic activity (*2*). The enzyme is designed to sense and adjust its activity according to the fluctuating levels of intracellular free Ca^{2+} in the outer segments of rods and cones. The fluctuation, in turn, regulates the concentration of the cyclic GMP pool, which gates the cation channels. Since Ca^{2+} enters the cell via the cGMP-gated channels and is extruded via the Na^+/Ca^{2+}, K^+ exchanger, the Ca^{2+} levels and ROS-GC1 activity are interlocked in phototransduction. In the present study the effect of CORD6 mutations on the modulation of ROS-GC1 phototransduction and the synaptic activity components has been analyzed. On the basis of these findings, an attempt has been made to define the phenotype of each dystrophy in molecular terms. The effects of each mutation on different aspects of visual transduction in an otherwise competent retina have been analyzed. The study has revealed several intriguing aspects, which are discussed under the following headings.

Phototransduction: (A) Dark Current. A basic operational principle of the phototransduction machinery is the maintenance of the optimum level of cytoplasmic cyclic GMP in the dark state. This keeps fractional (~5%) cyclic GMP channels open (*2*). The estimated cyclic GMP is ~4 μM, resulting from its balanced synthesis and hydrolysis. The E786D mutation has no influence on the intrinsic ROS-GC1 activity. Thus, the dark state of the photoreceptors would not be affected.

In contrast to the E786D mutation, the R787C mutation reduces the intrinsic ROS-GC1 activity by about 4-fold. Only one-fourth of the required cyclic GMP is produced. This would result in a lowered steady-state level of cyclic GMP

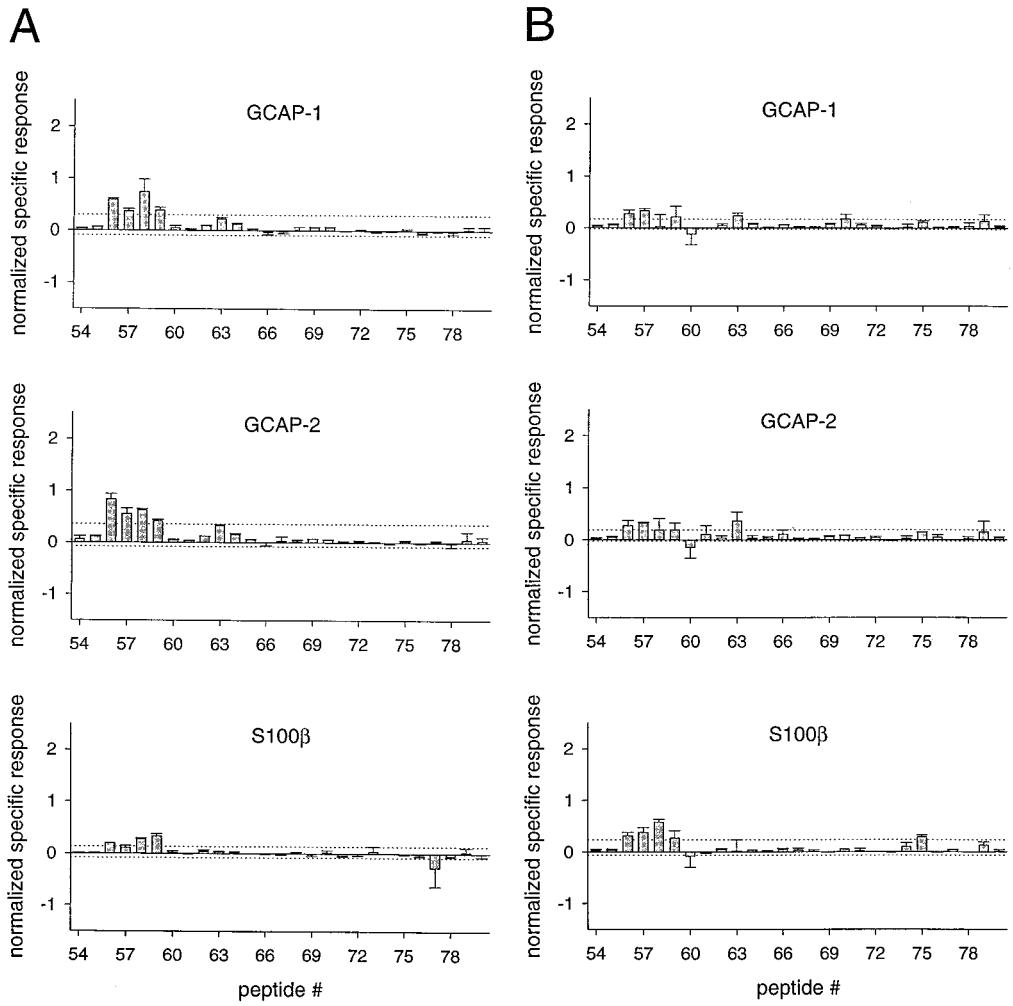

FIGURE 5: Binding of ROS-GC1 peptides to immobilized GCAP1, GCAP2, and S100β in the absence of Ca^{2+} (A) and in the presence of Ca^{2+} (B). Ca^{2+}-binding proteins were immobilized via thiol coupling as described under Materials and Methods. Peptides were applied in running buffer containing 1 nM free Ca^{2+} (A) or 24 μM free Ca^{2+} (B). Maximal amplitudes of binding signals were determined and normalized to a pulse of 1% glycerol. Nonspecific binding to a control surface was subtracted. Binding signals are expressed as normalized specific response. All runs were performed in duplicate. Dotted lines indicate the standard deviation of the overall mean.

in dark-adapted photoreceptor cell. This, in turn, will drastically reduce the open state of the cyclic GMP-gated channels, causing a reduction in dark current in the photoreceptors. Concomitant with the reduction of dark current is a decrease of cytoplasmic Ca^{2+} due to the operation of the exchanger. However, this fall in cytoplasmic Ca^{2+} would not be caused by light but by the defects of the R787C mutant (vide infra). An affected photoreceptor cell would sense a kind of light-adapted status, although it is in the dark state. The lowered Ca^{2+} level will in turn trigger the Ca^{2+}-dependent feedback signals by the Ca^{2+}-sensors—GCAP1, GCAP2, recoverin, and calmodulin. Thus, the mutant photoreceptor would adapt at lower light intensities for a given background light than normal cells. This will cause a shift in the response−intensity curve to lower light intensities. The affected individuals will, therefore, suffer from poor vision in bright light. This is, indeed, an affliction observed in CORD6 patients (*24*).

(B) GCAP1 Signaling. The R787C mutation makes ROS-GC1 hyperactive to modulation by GCAP1. The lower basal activity of the R787C mutant is fully compensated by this increased response to GCAP1. This would, however, lead to a dramatic change in the cGMP homeostasis in an affected cell. Thus, the cyclase mutation is predicted to have two physiological consequences: (1) It would greatly accelerate the recovery phase, and (2) it would compensate for the lower basal cyclase activity by increasing the GCAP1-dependent amplitude of modulation. The mutation has tricked the cyclase: the recovery phase would be greatly shortened and the photoreceptor would be put in a sustained state of "false" photoexcitation.

Both E786D and R787D are adjacent to each other, occurring in the predicted dimerization domain of the cyclase. Yet the E786D mutation affects neither the basal nor the GCAP1-dependent cyclase activity. However, both of these activities are affected by the R787C mutation. The change from E to D is very conservative and is anticipated to cause little configurational change in the cyclase, and hence, also in its basal and activated states. The mutation at residue 787 involves an R to C change, which is drastic. The change involves transformation of a charged residue to a hydrophobic residue, which, in turn, is highly reactive due to its sulfhydryl group. Normal catalysis of cGMP formation occurs at a dimer interface (*43*) and a very recent study has shown that activation by GCAPs involves the dimerization of ROS-GC1 (*44*). Apparently, the dimer formation is disturbed in the R787C mutant, leading to lower cyclase activity. Modulation by GCAP1 would then facilitate the

formation of the correct dimer interface in the mutant resulting in the observed 25-fold activation of ROS-GC1. That the mutation, indeed, affects the dimerization step and does not affect the GCAP1 binding step is in accord with the results of this study, where SPR screening shows that the hypothetical dimerization domain of ROS-GC1 does not contain the GCAP binding domain.

(C) GCAP2 Signaling. At a biochemical level, an extremely intriguing finding of this study relates to the GCAP2 activation of E786D mutant, without having much effect on the R787C mutant. This indicates that the E786D mutation selectively turns "on" the GCAP2 switching cyclase mechanism. This also indicates that GCAP1 and GCAP2 act at two different sites in ROS-GC1, supporting the same previous conclusion, which was based on the biochemical studies involving hybrid technology (*25*, *34*).

At a physiological level, consequences of the selective alteration of GCAP2 switch in E786D are difficult to interpret. The immunocytochemical presence of GCAP2 has been shown both in the rods and in the cones (*45*); however, no conclusive view has been reached about the precise role of GCAP2 in rods and cones. Factoring this in with the information that CORD6-linked ROS-GC1 mutations are primarily related first to the cone and then to the rod dystrophy (*24*), the cone GCAP2 in E786D dystrophy will accelerate the recovery phase. But it will have no effect in the R787C dystrophy.

Retinal Synapse. ROS-GC1 has also a putative role in retinal synaptic activity. The present study shows that the R787C mutation in ROS-GC1 also disables the activation of the enzyme by S100β. The S100β-dependent cyclase activity is halved in the mutant. Because the mutant in its basal state is only one-fourth as active as the wild type, this indicates that about 90% of the synaptic cyclase component has been damaged. It is, therefore, predicted that the synapse-related retinal functions in the individuals with this mutation will be severely affected. This prediction is in accord with a recent study where a cone−rod photoreceptor dystrophy has been related to a distortion of cone photoreceptor pedicles (*46*).

In conclusion, this study, for the first time, has shown the precise biochemical effects of two ROS-GC1-linked cone−rod dystrophies that cause significant damage in phototransduction and, presumably, at the retinal synapse. The findings have been applied to define the disease phenotypes in exact molecular terms.

ACKNOWLEDGMENT

We thank Mrs. Joan Sharma for help in the preparation of the manuscript. We also thank the anonymous reviewer for the stimulating and constructive criticism of the manuscript.

REFERENCES

1. Pugh, E. N., Jr., and Lamb, T. D. (1993) *Biochim. Biophys. Acta 1141*, 111−149.
2. Pugh, E. N., Jr., Duda, T., Sitaramayya, A., and Sharma, R. K. (1997) *Biosci. Rep. 17*, 429−473.
3. Koch, K.-W., and Stryer, L. (1988) *Nature 334*, 64−66.
4. Pugh, E. N., Jr., and Lamb, T. D. (1990) *Vis. Res. 30*, 1923−1948.
5. Ratto, G. M., Payne, R., Owen, W. G., and Tsien, R. Y. (1988) *J. Neurosci. 8*, 3240−3246.
6. Korenbrot, J. I., and Miller, D. L. (1989) *Vis. Res. 29*, 939−948.
7. Schnetkamp, P. P., and Bownds, M. D. (1987) *J. Gen. Physiol. 89*, 481−500.
8. Lagnado, L., Cervetto, L., and McNaughton, P. A. (1992) *J. Physiol. 455*, 111−142.
9. Gray-Keller, M. P., and Detwiler, P. B. (1994) *Neuron 13* (4), 849−861.
10. Kutty, R. K., Fletcher, R. T., Chader, G. J., and Krishna, G. (1992) *Biochem. Biophys. Res. Commun. 182*, 851−857.
11. Ahmad, I., and Barnstable, C. J. (1993) *Exp. Eye Res. 56*, 51−62.
12. Duda, T., Goraczniak, R. M., Sitaramayya, A., and Sharma, R. K. (1993) *Biochemistry 32*, 1391−1395.
13. Goraczniak, R. M., Duda, T., Sitaramayya, A., and Sharma, R. K. (1994) *Biochem. J. 302*, 455−461.
14. Yang, R. B., Foster, D. C., Garbers, D. L., and Fulle, H. J. (1995) *Proc. Natl. Acad. Sci. U.S.A. 92*, 602−606.
15. Shyjan, A. W., de Sauvage, F. J., Gillett, N. A., Goeddel, D. V., and Lowe, D. G. (1992) *Neuron 9*, 727−737.
16. Lowe, D. G., Dizhoor, A. M., Liu, K., Gu, Q., Spencer, M., Laura, R., Lu, L., and Hurley, J. B. (1995) *Proc. Natl. Acad. Sci. U.S.A. 92*, 5535−5539.
17. Goraczniak, R. M., Duda, T., and Sharma, R. K. (1997) *Biochem. Biophys. Res. Commun. 234*, 666−670.
18. Duda, T., Goraczniak, R., Surgucheva, I., Rudnicka-Nawrot, M., Gorczyca, W. A., Palczewski, K., Sitaramayya, A., Baehr, W., and Sharma, R. K. (1996) *Biochemistry 35*, 8478−8482.
19. Margulis, A., Goraczniak, R. M., Duda, T., Sharma, R. K., and Sitaramayya, A. (1993) *Biochem. Biophys. Res. Commun. 194*, 855−861.
20. Koch, K.-W., Stecher, P., and Kellner, R. (1994) *Eur. J. Biochem. 222*, 589−595.
21. Camuzat, A., Rozet, J.-M., Dollfus, H., Gerber, S., Perrault, I., Weissenbach, J., Munnich, A., and Kaplan, J. (1996) *Hum. Genet. 97*, 798−801.
22. Semple-Rowland, S. L, Lee, N. R., Van Hooser, J. P., Palczewski, K., and Baehr, W. (1998) *Proc. Natl. Acad. Sci. U.S.A. 95*, 1271−1276.
23. Duda, T., Venkataraman, V., Goraczniak, R., Lange, C., Koch, K.-W., and Sharma, R. K. (1999) *Biochemistry 38*, 509−515.
24. Kelsell, R. E., Gregory-Evans, K., Payne, A. M., Perrault, I., Kaplan, J., Yang, R.-B., Garbers, D. L., Bird, A. C., Moore, A. T., and Hunt, D. M. (1998) *Hum. Mol. Genet. 7*, 1179−1184.
25. Krishnan, A., Goraczniak, R., Duda, T., and Sharma, R. K. (1998) *Mol. Cell. Biochem. 178*, 251−259.
26. Gorczyca, W. A., Gray-Keller, M. P., Detwiler, P. B., and Palczewski, K. (1994) *Proc. Natl. Acad. Sci. U.S.A. 91*, 4014−4018.
27. Palczewski, K., Subbaraya, I., Gorczyca, W. A., Helekar, B. S., Ruiz, C. C., Ohguro, H., Huang, J., Zhao, X., Crabb, J. W., Johnson, R. S., Walsh, K. A., Gray-Keller, M. P., Detwiler, P., and Baehr, W. (1994) *Neuron 13*, 395−404.
28. Frins, S., Bonigk, W., Muller, F., Kellner, R., and Koch, K.-W. (1996) *J. Biol. Chem. 271*, 8022−8027.
29. Dizhoor, A. M., Lowe, D. G., Olshevskaya, E. V., Laura, R. P., and Hurley, J. B. (1994) *Neuron 12*, 1345−1352.
30. Dizhoor, A. M., Olshevskaya, E. O., Henzel, W. J., Wong, S. C., Stults, J. T., Ankoudinova, I., and Hurley, J. B. (1995) *J. Biol. Chem. 270*, 25200−25206.
31. Pozdnyakov, N., Yoshida, A., Cooper, N. G., Margulis, A., Duda, T., Sharma, R. K., and Sitaramayya, A. (1995) *Biochemistry 34*, 14279−14283.
32. Duda, T., Goraczniak, R. M., and Sharma, R. K. (1996) *Biochemistry 35*, 6263−6266.
33. Pozdnyakov, N., Goraczniak, R., Margulis, A., Duda, T., Sharma, R. K., Yoshida, A., and Sitaramayya, A. (1997) *Biochemistry 36*, 14159−14166.
34. Goraczniak, R., Duda, T., and Sharma, R. K. (1998) *Biochem. Biophys. Res. Commun. 245*, 447−453.

35. Sambrook, M. J., Fritsch, E. F., and Maniatis, T. (1989) *Molecular Cloning: A Laboratory Manual*, Cold Spring Harbor Laboratory Press, Cold Spring Harbor, NY.
36. Paul, A. K., Marala, R. B., Jaiswal, R. K., and Sharma, R. K. (1987) *Science 235*, 1224−1226.
37. Nambi, P., Aiyar, N. V., Roberts, A. N., and Sharma, R. K. (1982) *Endocrinology 111*, 196−200.
38. Schrem, A., Lange, C., Beyermann, M., and Koch, K.-W. (1999) *J. Biol. Chem. 274*, 6244−6249.
39. Lange, C., and Koch, K.-W. (1997) *Biochemistry 36*, 12019−12026.
40. Yang, R.-B., Fulle, H.-J., and Garbers, D. L. (1996) *Genomics 31*, 367−372.
41. Johnston, J. P., Farhangfar, F., Aparicio, J. G., Nam, S. H., and Applebury, M. (1997) *Gene 193*, 219−227.
42. Duda, T., Venkataraman, V., Krishnan, A., and Sharma, R. K. (1998) *Mol. Cell. Biochem. 189*, 63−70.
43. Liu, Y., Ruoho, A. E., Rao, V. D., and Hurley, J. H. (1997) *Proc. Natl. Acad. Sci. U.S.A. 94*, 13414−13419.
44. Yu, H., Olshevskaya, E., Duda, T., Seno, K., Hayashi, F., Sharma, R. K., Dizhoor, A. M., and Yamazaki, A. (1999) *J. Biol. Chem. 274*, 15547−15555.
45. Howes, K., Bronson, J. D., Dang, Y. L., Li, N., Zhang, K., Ruiz, C., Helekar, B., Lee, M., Subbaraya, I., Kolb, H., Chen, J., and Baehr, W. (1998) *Invest. Ophthalmol. Vis. Sci. 39*, 867−875.
46. Gregory-Evans. K., Fariss. R. N., Possin, D. E., Gregory-Evans, C. Y., and Milam, A. H. (1998) *Ophthalmology 105*, 2306−2312.

BI9915972